66 *KSME International Journal, Vol. 15, No. 1, pp. 66~80, 2001*

# Electronic Control of Braking Force Distribution for Vehicles Using a Direct Adaptive Fuzzy Controller

**Seungdae Kim**
*Graduate School, Sungkyunkwan University*
**Hunmo Kim***
*School of Mechanical Engineering, Sungkyunkwan University*
**Yoon-Gyeoung Sung**
*School of Mechanical Engineering, Yeungnam University*

In brake systems, a proportioning valve(P. V), which reduces the brake line pressure on each wheel cylinder for the anti-locking of rear wheels, is closely related to the safety of vehicles. However, it is impossible for current P. V. s to completely control brake line pressure because, mechanically, it is an open loop control system. In this paper we describe an electronic brake force distribution system using a direct adaptive fuzzy controller in order to completely control brake line pressure using a closed loop control system. The objective of the electronic brake force distribution system is to change the cut-in-pressure and the valve slop of the P. V in order to obtain better performance of the brake system than with mechanical systems.

**Key Words** : Direct Adaptive Fuzzy Controller, Braking Force Distribution, Proportioning Valve(P. V), Load Sensing Proportioning Valve(L. S. P. V)

**Nomenclature**

| | |
|---|---|
| $\chi$ | : Center of gravity height divided by wheelbase |
| $\Psi$ | : Ratio of static rear axle load to total weight |
| $\mu_{TF}$ | : Front traction coefficient |
| $\mu_{TR}$ | : Rear traction coefficient |
| $F_{ZF}$ | : Static load on front axle, kgf |
| $F_{ZR}$ | : Static load on rear axle, kgf |
| $F_{ZF,dyn}$ | : Dynamic load on front axle, kgf |
| $F_{ZR,dyn}$ | : Dynamic load on rear axle, kgf |
| $F_{XF,ideal}$ | : Ideal braking force of front, kgf |
| $F_{XR,ideal}$ | : Ideal braking rear of rear, kgf |
| W | : Vehicle weight, kgf |
| $B_F$ | : Actual braking force of front, kgf |
| $B_R$ | : Actual braking force of rear, kgf |
| $BEF_F$ | : Friction coefficient of front |
| $BEF_R$ | : Friction coefficient of rear |
| $P_F$ | : Braking pressure of front, kgf/cm$^2$ |
| $P_R$ | : Braking pressure of rear, kgf/cm$^2$ |
| $P_{F,Loss}$ | : Braking pressure loss of front, kgf/cm$^2$ |
| $P_{R,Loss}$ | : Braking pressure loss of rear, kgf/cm$^2$ |
| $A_{WF}$ | : Wheel cylinder area of front, mm |
| $A_{WR}$ | : Wheel cylinder area of rear, mm |
| $\eta$ | : Effective coefficient |
| $R_F$ | : Effective braking radius of front |
| $R_R$ | : Effective braking radius of rear |
| $r_F$ | : Radius of front tire |
| $r_R$ | : Radius of rear tire |

* Corresponding Author,
**E-mail** : kimhm@me.skku.ac.kr
**TEL** : +82-31-290-7450 ; **FAX** : +82-31-290-5849
School of Mechanical Engineering, Sungkyunkwan University, 300, Chunchun-dong, Jangan-gu, Suwon, Kyonggi-do 440-746, Korea. (Manuscript **Received** July 25, 2000; **Revised** October 18, 2000)

## 1. Introduction

As the automobile industry develops, manufacturers are able to supply products that are safer, more convenient, and more powerful. In the case of automobile systems, the body, chassis, and powertrain systems are becoming electronic. As a result, current systems can be controlled more delicately(BOSCH, 1993; Jurgen, 1997; Mizutani, 1992). Located in the chassis, the brake system is by far the most important mechanism in any vehicle, because the safety and lives of those riding in the vehicle depend on the proper operation of the brake system. Designers should therefore consider safety and efficiency when they design brake systems. When the brake system operates, there is an important occurrence, defined by Newton's dynamics as load transfer, which reduces the rear axle load. The load transfer results in rear wheel locking before front wheel locking. Modern automobiles use a proportroning valve (P. V) that prevents rear wheel locking before front wheel locking so as to secure the ability to steer the vehicle. The P. V. reduces the rear brake line pressure at a fixed ratio above its cut-in-pressure. The P. V. is controlled by its inner spring force and by the difference between cross sections. But this system cannot actively adjust for the weight change of a vehicle. If the weight change of a vehicle becomes greater, the loss of braking force increases(Kim, 1997; Giuseppe, 1970; Rudolf, 1971; 1974). In the case of commercial vehicles, where weight change is great, a load sensing proportioning valve (L. S. P. V) is used. Its pressure reducing ratio is equal to the ratio of the P. V., but it can change the cut-in -pressure using a linkage system. So, the L. S. P. V. is more efficient than the P. V. in the case of commercial vehicles.

However, this mechanical system has some weaknesses which are described below (Hiroyuki, 1977; Frederic, 1969; Gunther, 1992):

1) The pressure cannot be controlled exactly.

2) The mechanical system cannot change its pressure reducing ratio freely.

3) In other vehicles, the weight may vary. So, we cannot use a common system, and it is difficult to assemble vehicle-specific systems.

In this paper we propose a new electronic system which can change the pressure reducing ratio and the cut-in-pressure using a direct adaptive fuzzy controller to overcome the weaknesses of the mechanical system. We also propose a hardware system including sensors, a reducing valve, and a control unit to change the system from mechanical to electronic. Additionally, we propose a direct adaptive fuzzy algorithm in which the fuzzy rule base is changed automatically depending on the deceleration conditions and weight conditions.

## 2. Braking Dynamics

### 2.1 Ideal braking force

For a non-decelerating vehicle, the static axle load distribution is defined by the ratio of static rear axle load to the total vehicle weight, as follows:

$$\Psi = F_{ZR}/W \tag{1}$$

The relative static front axle load is given by

$$1-\Psi = F_{ZF}/W \tag{2}$$

Whenever the brakes are applied in a forward moving vehicle, the weight of the vehicle is transferred forward. The forces acting on a two-axle vehicle which is decelerating are illustrated in Fig. 1. The dynamic normal forces on the front axle and the rear axle respectively are defined as follows:

$$F_{ZF,dyn} = (1-\Psi+\chi a)W \tag{3}$$

$$F_{ZR,dyn} = (\Psi-\chi a)W \tag{4}$$

Multiplication of the dynamic axle load by the traction coefficients yields the dynamic braking forces for the front axle and the rear axle, respectively:

$$F_{XF} = (1-\Psi+\chi a)W\mu_{TF} \tag{5}$$

$$F_{XR} = (\Psi-\chi a)W\mu_{TR} \tag{6}$$

We call the braking force which is required for each brake the ideal braking force. The ideal braking forces may be determined by setting the traction coefficient equal to vehicle deceleration in Eqs. (5) and (6), resulting in the ideal braking

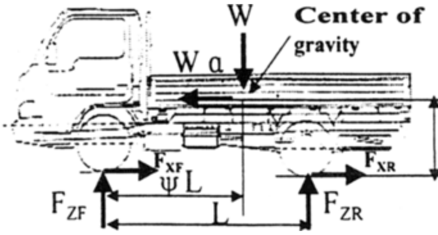


**Fig. 1** Dynamic forces acting on a decelerating vehicle

forces for the front axle and the rear axle, respectively:

$$F_{XF,ideal}=(1-\Psi+\chi a)Wa \tag{7}$$
$$F_{XR,ideal}=(\Psi-\chi a)Wa \tag{8}$$

These forces depend on the vehicle's weight change. Inspection of Eqs. (7) and (8) indicates a quadratic relationship relative to deceleration $a$. In braking, the amount of load transfer off the rear axle (and onto the front axle) is symbolized by the term $\chi_a$.

### 2.2 Actual braking force

The actual braking force is produced by the hydraulic brake system installed in the vehicle. This force, however, is not equal to the ideal braking force because of mechanical limits (Frederic, 1969; Gunther, 1992; Rudolf, 1992; Thomas, 1992).

The brake line pressure which is obtained by the master cylinder is transferred to the front and rear wheel cylinders. The pressure generates the actual braking force from the friction between pads and discs in the front wheels and between drums and shoes in the rear wheels. This mechanism is shown in Fig. 2.

The actual braking force may be obtained from Eqs. (9) and (10):

$$B_F=\frac{2\times BEF_F\times(P_F-P_{F,LOSS})\times A_{WF}\times\eta\times R_F}{r_F} \tag{9}$$
$$B_R=\frac{2\times BEF_R\times(P_R-P_{R,LOSS})\times A_{WR}\times\eta\times R_R}{r_R} \tag{10}$$

Inspection of Eqs. (9) and (10) indicates a linear relationship relative to the brake line pressure.

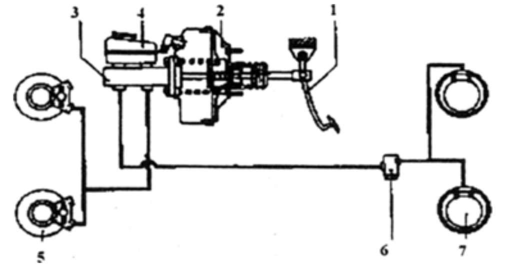


1. Brake pedal 2. Master vac. 3. Master cylinder
4. Brake oil reserve tank 5. Disc brake
6. P. V OR L.S.P.V 7. Drum brake

**Fig. 2** Configuration of normal hydraulic brake system

Additionally, the difference between the ideal braking force and the actual braking force results in poor braking efficiency and a longer overall stopping distance.

### 2.3 Braking forces in mechanical systems

As mentioned above, the rear axle load becomes lighter during braking, so relatively less brake line pressure is required on the rear brakes to keep them from locking before the front brakes. Hence, vehicles need a system that reduces rear brake line pressure. There are two basic types of valves which reduce rear brake line pressure, namely P. V. and L. S. P. V. The P. V. is used on vehicles without weight change. A typical schematic of the P. V. is shown in Fig. 3. The rear brake line pressure is equal to the front brake line pressure until the rear brake line pressure reaches the cut-in-pressure. After the cut-in-pressure is reached, the P. V. reduces the rear brake line pressure in proportion to the valve slop.

The spring which is in the P. V. controls the cut-in-pressure, and the difference in area between Cup1 and Cup2 controls the valve slop. The braking force of a P. V. is shown in Fig. 4.

We can see that the loss of braking forces increases in proportion to weight. So, we can reduce the loss of braking forces by using an L. S. P. V. A typical schematic of the L. S. P. V is shown in Fig. 5.

An L. S. P. V is commonly used in commercial vehicles where weight change is great. In many light trucks the L. S. P. V. is added to the normal

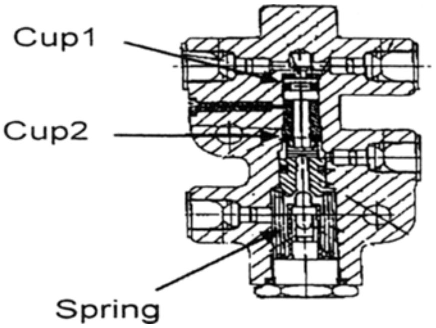


**Fig. 3** Schematic of P.V.

combination valve system such that it will further reduce the rear brake line pressure and cut-in-pressure when lightly loaded but be ineffective when loaded. So, the L. S. P. V. can achieve a greater reduction in the loss of brake forces than can the P. V. A typical graph of braking force in an L. S. P. V. is shown in Fig. 6.

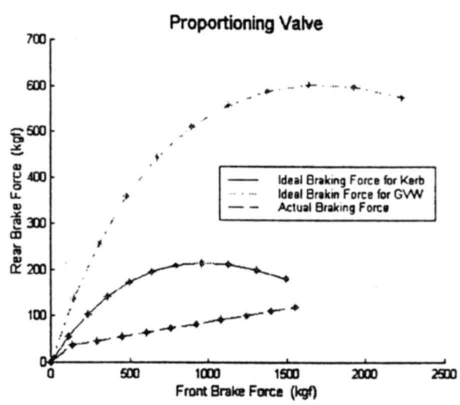


**Fig. 4** Braking force of a P.V.

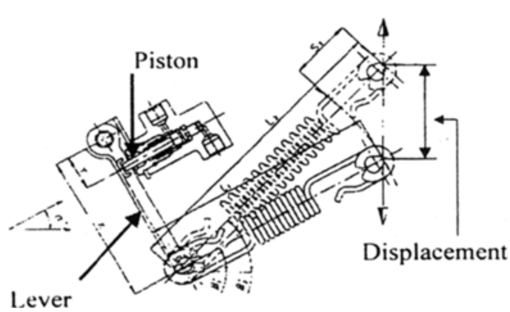


**Fig. 5** Schematic of L.S.P.V.

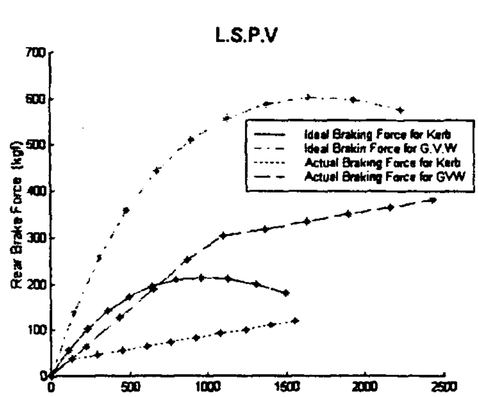


**Fig. 6** Braking force of L.S.P.V.

## 3. System Configuration

### 3.1 Hardware

The aims of our research are outlined below.

1) Converting the current L. S. P. V. into an electronic system.

2) Increasing braking efficiency.

3) Making an electronic system that is suitable for any vehicle.

A very important problem is how to sense the load and the brake line pressure, and to operate an electronic reducing valve. Also, the system requires a sensor to sense the deceleration.

Our new system has four parts, as shown in Fig. 7:

① Electronic reducing valve : It controls the cut-in-pressure and the reducing ratio by using a solenoid piston. It is shown in Fig. 8.

② Direct adaptive fuzzy controller : It takes

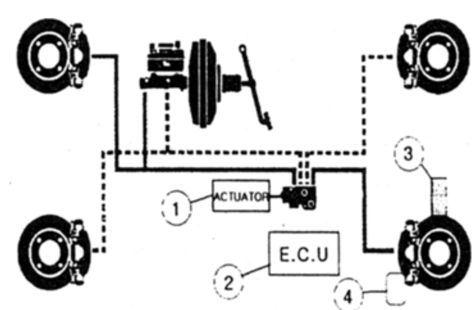


① Electronic reducing valve
② Direct adaptive fuzzy controller
③ Load cell & deceleration sensor
④ Braking pressure sensor

**Fig. 7** Configuration of an electronic L.S.P.V. system

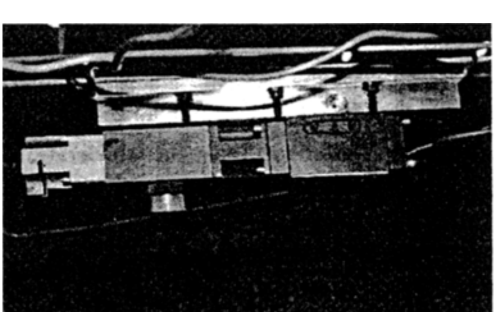

**Fig. 8** Electronic reducing valve

**Fig. 9** Direct adaptive fuzzy controller

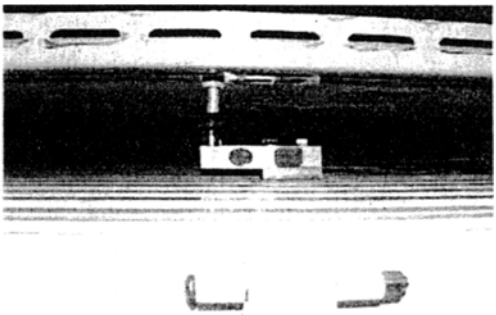

**Fig. 10** Load cell

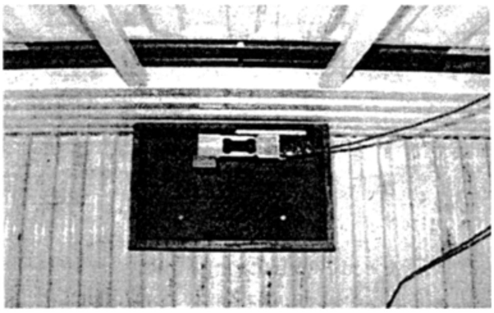

**Fig. 11** Deceleration sensor

signals from each sensor and controls the electronic reducing valve to change the cut-in-pressure and the reducing ratio of the electronic reducing valve. It is shown in Fig. 9.

③ Load cell & deceleration sensor : The former measures the change in weight. It is shown in Fig. 10. The latter measures the deceleration of the vehicle when braking in order to calculate the reference brake line pressure of the rear brakes. It is shown in Fig. 11.

④ Brake line pressure sensor : It measures the pressure in the brake lines and calculates the brake line pressure error when braking. It is shown in Fig. 12.

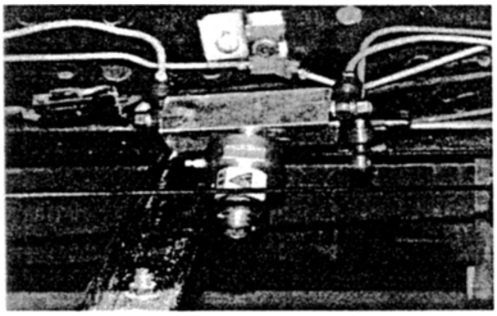

**Fig. 12** Brake line pressure sensor

The total system operates as follows. First, signals come from each sensor. Then, the controller calculates the proper cut-in-pressure and the valve slop to minimize the braking force loss. If the rear brake line pressure is greater than the proper cut-in-pressure, then the controller operates the electronic valve which reduces the rear brake line pressure. Also, the controller calculates the pressure error with signals from the pressure sensors.

### 3.2 Direct adaptive fuzzy control

Basically, it is difficult to model and simulate complex real-world systems for control systems development. Even if a relatively accurate model of a dynamic system can be developed, it is often too complex to use in controller development, especially for many conventional control design procedures that require restrictive assumptions for the plant. It is for this reason that in practice conventional controllers are often developed via simple models of the plant behavior that satisfy the necessary assumptions. So, in many cases, control designers use a fuzzy controller in order to control the plant exactly (Zadeh, 1973; 1985). But, if any parameters influence the input signal and the environment or if unpredictable cases exist, then we cannot use a fuzzy controller.

It is for this reason that we need a way to automatically tune the fuzzy controller so that it can adapt to different plant conditions. This adaptive mechanism observes the signals from the control system and adapts the parameters of the controller to maintain performance even if there are changes in the plant. If a model of the plant

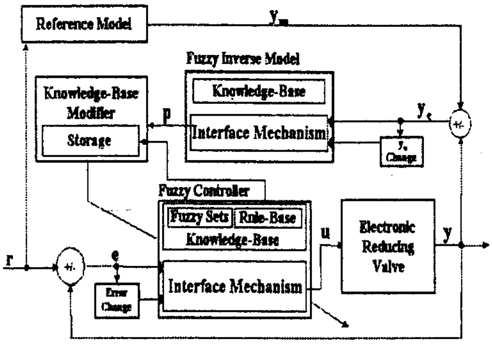


**Fig. 13** Direct adaptive fuzzy controller

exists, we refer to the controller as a direct adaptive fuzzy controller (Lefteri and Robert, 1997; Kevin and Stephen, 1998; Layne and Kevin, 1993; 1996; Li, 1994). The schematic of the direct adaptive fuzzy controller is shown in Fig. 13. We used a direct adaptive fuzzy controller as a controller in our proposed system.

### 3.2.1 FMRLC

We used an FMRLC (fuzzy model reference learning control) algorithm for direct adaptive fuzzy controller in order to improve the performance of the closed-loop system by generating command inputs to the plant and utilizing feedback information from the plant. The FMRLC has four parts: the plant, the fuzzy controller to be tuned, the reference model, and the learning mechanism. The error and the error change between the reference model and the plant output distinguish an FMRLC from a fuzzy control.

The learning mechanism can be discribed as follows:

① The fuzzy inverse model performs the function of mapping $y_e(kT)$ (representing the deviation from the desired behavior) to change in the process inputs $p(kT)$ that are necessary to force $y_e(kT)$ to zero.

② The knowledge base modifier performs the function of modifying the fuzzy controller's rule base to affect the needed changes in the process inputs.

The error and error change are shown below:

$$e(kT)=r(kT)-y(kT) \tag{11}$$

$$c(kT)=\frac{e(kT)-e(kT-T)}{T} \tag{12}$$

where $T$ is the sampling time and $k$ is the sampling number.

The fuzzy rule-base is defined as follows:

$$\text{IF } \tilde{e} \text{ is } E^i \text{ AND } \tilde{c} \text{ is } C^l \text{ THEN } \tilde{u} \text{ is } U^m \tag{13}$$

where $e$ and $c$ denote the linguistic variables associated with controller inputs $e(kT)$ and $c(kT)$, respectively, $U$ denotes the linguistic variable associated with the controller output $u$, and $E^j$ and $C^l$ denote the $j$th ($l$th) linguistic value associated with $e$ and $c$, respectively.

### 3.2.2 Learning mechanism

The learning mechanism consists of two parts: a fuzzy inverse model and a rule-base modifier. The variables of the fuzzy inverse model are $y_e$ (representing the error between the reference model and the plant output) and $y_c$ (representing the error change). The $y_e$ and $y_c$ have 11 fuzzy sets, respectively. The fuzzy number is of the triangular type.

The output of the fuzzy inverse model is $p$. The center of rules will be shifted by the $p$. The $y_e$ and $y_c$ are defined below:

$$y_e(kT)=y_m(kT)-y(kT) \tag{14}$$

$$y_c(kT)=\frac{y_e(kT)-y_e(kT-T)}{T} \tag{15}$$

where $T$ is the sampling time and $k$ is the sampling number.

The fuzzy rule-base for calculating the output $p$ in the fuzzy inverse model is shown below:

$$\text{IF } \tilde{y}_e \text{ is } Y_e^j \text{ AND } \tilde{y}_c \text{ is } Y_c^l \text{ THEN } \tilde{p} \text{ is } P^m \tag{16}$$

where $Y_e^j$ and $Y_c^l$ are linguistic values.

The output $p$ adapts the fuzzy controller, using the equation below and employing the fuzzy modifier:

$$c_i(kT)=c_i(kT-dT)+p(kT) \tag{17}$$

where $c_i$ is the center of the fuzzy membership function for the $i$th output variable at $kT$.

The input values should be normalized so that the fuzzy controller can recognize them. Fuzzification is needed to change the normalized input values into linguistic variables. In our research, we conduct the fuzzification using membership functions that are of the triangular type because they are easier to calculate.

The linguistic values for the input and output are shown below:

1) Input variable

① The error of the rear brake line pressure

The linguistic value for the error of the rear brake line pressure is $e$ (error). It is normalized between -1 and 1. The membership function for the error is shown in Fig. 14.

② The error change of rear brake line pressure

The linguistic value for the error change of the rear brake line pressure is $c$ (error change). It is normalized between -1 and 1. The membership function for the error change is shown in Fig. 15.

2) Output variable

The linguistic value for the output variable which is the input voltage of the electronic reducing valve is u. It is normalized between -1 and 1. The membership function for the output is shown in Fig. 16.

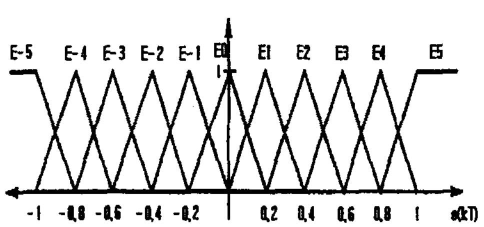


**Fig. 14** Membership functions for error unyierse of discourse

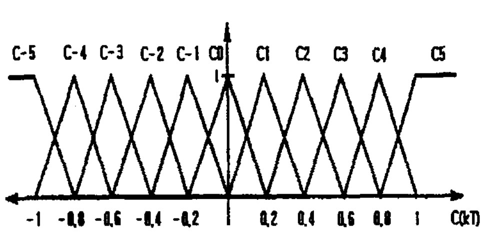


**Fig. 15** Membership functions for error change universe of discourse

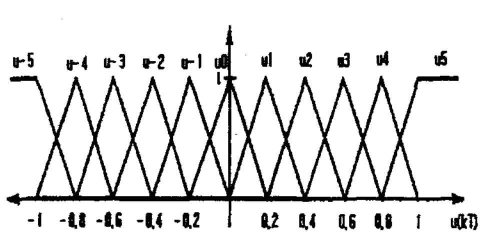


**Fig. 16** Membership functions for output universe of discourse

3) Rule-base

The rule-base for the fuzzy controller that controls the rear brake line pressure has rules of the form "IF-THEN".

> R : *IF (Pressure Error) is Zero and (Pressure Error Change) is Zero*
> *THEN (Change of Valve Voltage) is Zero,*

where zero is a linguistic value for the input and output. The input variables have 11 membership functions. So, the rule-base has 121 rules. The rule-bases for the fuzzy controller are shown in Table 1 and the rule-bases for the fuzzy inverse model are shown in Table 2.

**Table 1** Fuzzy rule-base

| e \ c | −1 | −0.8 | −0.6 | −0.4 | −0.2 | 0 | 0.2 | 0.4 | 0.6 | 0.8 | 1 |
|---|---|---|---|---|---|---|---|---|---|---|---|
| −1 | −1 | −1 | −1 | −1 | −1 | −1 | −0.8 | −0.6 | −0.4 | −0.2 | 0 |
| −0.8 | −1 | −1 | −1 | −1 | −1 | −0.8 | −0.6 | −0.4 | −0.2 | 0 | 0.2 |
| −0.6 | −1 | −1 | −1 | −1 | −0.8 | −0.6 | −0.4 | −0.2 | 0 | 0.2 | 0.4 |
| −0.4 | −1 | −1 | −1 | −0.8 | −0.6 | −0.4 | −0.2 | 0 | 0.2 | 0.4 | 0.6 |
| −0.2 | −1 | −1 | −0.8 | −0.6 | −0.4 | −0.2 | 0 | 0.2 | 0.4 | 0.6 | 0.8 |
| 0 | −1 | −0.8 | −0.6 | −0.4 | −0.2 | 0 | 0.2 | 0.4 | 0.6 | 0.8 | 1 |
| 0.2 | −0.8 | −0.6 | −0.4 | −0.2 | 0 | 0.2 | 0.4 | 0.6 | 0.8 | 1 | 1 |
| 0.4 | −0.6 | −0.4 | −0.2 | 0 | 0.2 | 0.4 | 0.6 | 0.8 | 1 | 1 | 1 |
| 0.6 | −0.4 | −0.2 | 0 | 0.2 | 0.4 | 0.6 | 0.8 | 1 | 1 | 1 | 1 |
| 0.8 | −0.2 | 0 | 0.2 | 0.4 | 0.6 | 0.8 | 1 | 1 | 1 | 1 | 1 |
| 1 | 0 | 0.2 | 0.4 | 0.6 | 0.8 | 1 | 1 | 1 | 1 | 1 | 1 |

**Table 2** Fuzzy inverse model rule-base

| ye \ yc | −1 | −0.8 | −0.6 | −0.4 | −0.2 | 0 | 0.2 | 0.4 | 0.6 | 0.8 | 1 |
|---|---|---|---|---|---|---|---|---|---|---|---|
| −1 | −1 | −1 | −1 | −1 | −1 | −1 | −0.8 | −0.6 | −0.4 | −0.2 | 0 |
| −0.8 | −1 | −1 | −1 | −1 | −1 | −0.8 | −0.6 | −0.4 | −0.2 | 0 | 0.2 |
| −0.6 | −1 | −1 | −1 | −1 | −0.8 | −0.6 | −0.4 | −0.2 | 0 | 0.2 | 0.4 |
| −0.4 | −1 | −1 | −1 | −0.8 | −0.6 | −0.4 | −0.2 | 0 | 0.2 | 0.4 | 0.6 |
| −0.2 | −1 | −1 | −0.8 | −0.6 | −0.4 | −0.2 | 0 | 0.2 | 0.4 | 0.6 | 0.8 |
| 0 | −1 | −0.8 | −0.6 | −0.4 | −0.2 | 0 | 0.2 | 0.4 | 0.6 | 0.8 | 1 |
| 0.2 | −0.8 | −0.6 | −0.4 | −0.2 | 0 | 0.2 | 0.4 | 0.6 | 0.8 | 1 | 1 |
| 0.4 | −0.6 | −0.4 | −0.2 | 0 | 0.2 | 0.4 | 0.6 | 0.8 | 1 | 1 | 1 |
| 0.6 | −0.4 | −0.2 | 0 | 0.2 | 0.4 | 0.6 | 0.8 | 1 | 1 | 1 | 1 |
| 0.8 | −0.2 | 0 | 0.2 | 0.4 | 0.6 | 0.8 | 1 | 1 | 1 | 1 | 1 |
| 1 | 0 | 0.2 | 0.4 | 0.6 | 0.8 | 1 | 1 | 1 | 1 | 1 | 1 |

**Table 3** Vehicle specifications

| Spec. | Kerb | G.V.W. |
|---|---|---|
| Total Weight (kgf) | 1675 | 2805 |
| Frt. Axle Load (kgf) | 1075 | 1340 |
| Rr. Axle Load (kgf) | 600 | 1465 |
| Wheelbase (mm) | 2515 | |
| Gravity Center Height (mm) | 630 | 796.7 |

**Fig. 17** The 1-ton truck used for testing

## 4. Results

The simulation progressed from an empty weight condition, through a half weight condition, to a gross weight condition. We assumed that the test road had a constant friction coefficient on a flat, dry asphalt, and that deceleration was constant on the flat road. The weight conditions were selected as follows. The empty weight condition was 1840kg including driver weight, helper weight, all kinds of experimental devices, and the half weight condition was 2351kg. The gross weight condition was 2738kg. The loads were located uniformly on the deck of the vehicle. These assumptions were made in order to maintain uniform conditions in the experiments. For the simulation and the test, we selected a 1-ton truck. The test truck is shown in Fig. 17. Tables 3, 4 and 5 show the vehicle specifications, the brake system specifications, and the mechanical L. S. P. V. specifications, respectively. To compare the characteristics of reducing pressure according to changes in weight conditions, we demonstrated three cases: the empty weight condition, the half weight condition, and the gross weight condition.

**Table 4** Brake system specifications

| | Front | Rear |
|---|---|---|
| Effective Braking Radius (mm) | 100 | 110 |
| Brake Factor | 0.76 | 2.5 |
| Wheel Cylinder Diameter (mm) | 60.6 | 15.87 |
| Effective Tire Radius (mm) | 321 | 274 |
| Braking Efficiency | 0.95 | |
| Pressure Loss (kgf/cm$^2$) | 0.5 | |

**Table 5** Mechanical L. S. P. V specifications

| | Kerb | G.V.W |
|---|---|---|
| Cut-in-pressure (kgf/cm$^2$) | 10 | 80 |
| Valve Slop (%) | 20 | |

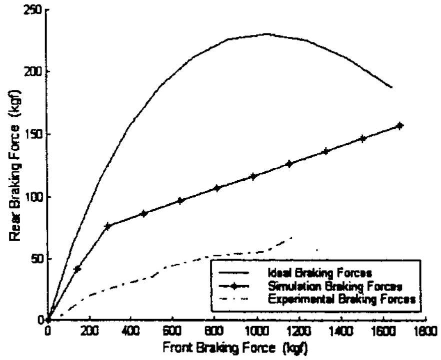


**Fig. 18** Mechanical system results of 1840kg

### 4.1 Simulation results

#### 4.1.1 Simulation results for the mechanical system

Figures 18, 19 and 20 show the braking force distribution simulation results for the empty weight condition, the half weight condition, and the gross weight condition, respectively. These results show that the mechanical system can improve braking force in accordance with changes in weight condition by changing the cut

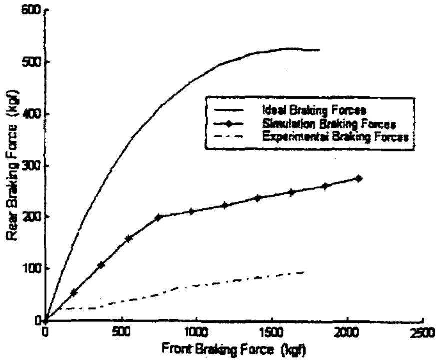


**Fig. 19** Mechanical system results for 2351kg

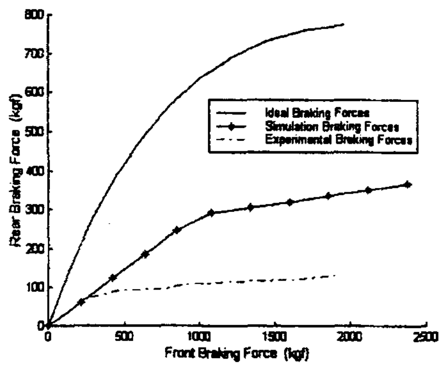


**Fig. 20** Mechanical system results for 2738kg

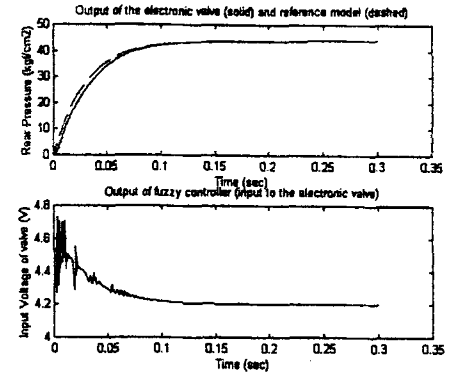


**Fig. 21** Simulation results of the direct adaptive fuzzy controller for 1840kg at 0.1g

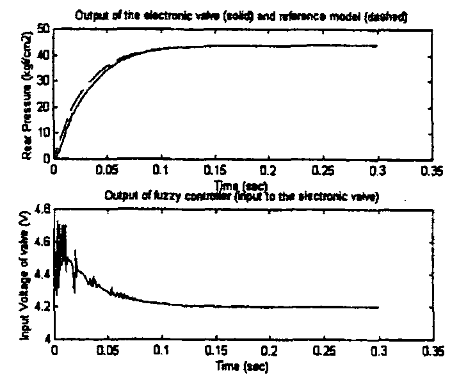


**Fig. 22** Simulation results of the direct adaptive fuzzy controller for 1840kg at 1.0g

-in-pressure of the L. S. P. V. Because this system causes a considerable gap between the ideal braking force and the actual braking force, there is a large loss of braking force in spite of changes in the cut-in-pressure.

### 4.1.2 Simulation result for the electronic system

The simulation conditions assumed that braking occurred over a short time (0.3 second on a flat, dry asphalt road), and that the deceleration of the vehicle was kept at a constant rate, because the braking force was transferred from the master cylinder to the wheel cylinder in 0.15 second. We considered two cases. The first involved changing the deceleration of the vehicle while the weight of the vehicle remained constant. The second involved changing the weight of the vehicle while the deceleration of the vehicle remained constant. The deceleration of the vehicle was divided into two cases: a low rate of deceleration of 0.1g, and a high rate deceleration of 1.0g.

1) Different deceleration, constant weight

The simulation results are shown in Figs. 21 and 22. From these results, we found that the output of the direct adaptive fuzzy controller followed the reference pressure line very well. The changes in the fuzzy rule-base for the low rate of deceleration of 0.1g and the high rate of deceleration of 1.0g are shown in Tables 6 and 7, respectively. In these tables, we found that most output variables of the rule-base were tuned from the original values of between $-1$ and 1 to zero. The zero implies that the learning mechanism does not need to tune the output variables of the controller. So, the more the output variables of zero increase, the less pressure error the system has. We also found that pressure error occurred when the error and the change in error were small in the center of the rule-base.

**Table 6** Changes in the fuzzy rule-base for 1840kg at 0.1g Time 0.3sec

| e \ c | −1 | −0.8 | −0.6 | −0.4 | −0.2 | 0 | 0.2 | 0.4 | 0.6 | 0.8 | 1 |
|---|---|---|---|---|---|---|---|---|---|---|---|
| −1 | 0 | 0 | 0 | 0 | 0 | 0 | 0 | 0 | 0 | 0 | 0 |
| −0.8 | 0 | 0 | 0 | 0 | 0 | 0 | 0 | 0 | 0 | 0 | 0 |
| −0.6 | 0 | 0 | 0 | 0 | 0 | 0 | 0 | 0 | 0 | 0 | 0 |
| −0.4 | 0 | 0 | 0 | 0 | 0 | 0 | 0 | 0 | 0 | 0 | 0 |
| −0.2 | 0 | 0 | 0 | 0 | 0 | 0 | 0 | 0 | 0 | 0 | 0 |
| 0 | 0 | 0 | 0 | −0.0096 | −0.0425 | 0.0000 | 0.0328 | 0 | 0 | 0 | 0 |
| 0.2 | 0 | 0 | 0 | −0.0244 | 0.0567 | 0.2356 | 0.0328 | 0 | 0 | 0 | 0.0269 |
| 0.4 | 0 | 0 | 0 | −0.0148 | 0.0992 | 0.2356 | 0 | 0 | 0 | 0 | 0.0269 |
| 0.6 | 0 | 0 | 0 | 0 | 0 | 0 | 0 | 0 | 0 | 0 | 0 |
| 0.8 | 0 | 0 | 0 | 0 | 0 | 0 | 0 | 0 | 0 | 0 | 0 |
| 1 | 0 | 0 | 0 | 0 | 0 | 0 | 0 | 0 | 0 | 0 | 0 |

**Table 7** Changes in the fuzzy rule-base for 1840kg at 1.0g Time 0.3sec

| e \ c | −1 | −0.8 | −0.6 | −0.4 | −0.2 | 0 | 0.2 | 0.4 | 0.6 | 0.8 | 1 |
|---|---|---|---|---|---|---|---|---|---|---|---|
| −1 | 0 | 0 | 0 | 0 | 0 | 0 | 0 | 0 | 0 | 0 | 0 |
| −0.8 | 0 | 0 | 0 | 0 | 0 | 0 | 0 | 0 | 0 | 0 | 0 |
| −0.6 | 0 | 0 | 0 | 0 | 0 | 0 | 0 | 0 | 0 | 0 | 0 |
| −0.4 | 0 | 0 | 0 | 0 | 0 | 0 | 0 | 0 | 0 | 0 | 0 |
| −0.2 | 0 | 0 | 0 | 0 | 0 | 0 | 0 | 0 | 0 | 0 | 0 |
| 0 | 0 | 0 | 0 | −0.0096 | −0.0425 | 0.0000 | 0.0328 | 0 | 0 | 0 | 0 |
| 0.2 | 0 | 0 | 0 | −0.0244 | 0.0567 | 0.2356 | 0.0328 | 0 | 0 | 0 | 0.0269 |
| 0.4 | 0 | 0 | 0 | −0.0148 | 0.0992 | 0.2356 | 0 | 0 | 0 | 0 | 0.0269 |
| 0.6 | 0 | 0 | 0 | 0 | 0 | 0 | 0 | 0 | 0 | 0 | 0 |
| 0.8 | 0 | 0 | 0 | 0 | 0 | 0 | 0 | 0 | 0 | 0 | 0 |
| 1 | 0 | 0 | 0 | 0 | 0 | 0 | 0 | 0 | 0 | 0 | 0 |

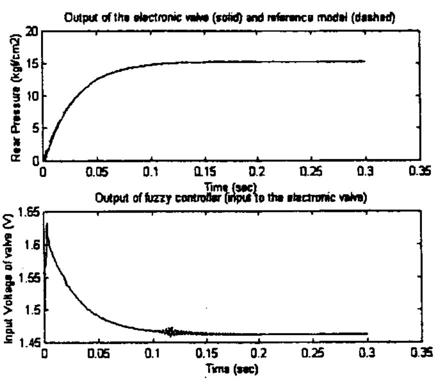


**Fig. 23** Simulation results of the direct adaptive fuzzy controller for 2351kg at 0.1g

2) Constant deceleration, different weight

The simulation results are shown in Figs. 23 and 24. From these results, we also found that the output of the direct adaptive fuzzy controller followed the reference pressure line very well. The changes in the fuzzy rule-base for the 2351kg -weight condition and the 2738kg-weight condition are shown in Tables 8 and 9, respectively. In these tables, we found that most output variables of the rule-base were tuned from the original values of between -1 and 1 to zero. We also found that pressure error occurred when the error and the change in error were small in the center of the

**Table 8** Changes in the fuzzy rule-base for 2351kg at 0.1g Time 0.3sec

| e \ c | −1 | −0.8 | −0.6 | −0.4 | −0.2 | 0 | 0.2 | 0.4 | 0.6 | 0.8 | 1 |
|---|---|---|---|---|---|---|---|---|---|---|---|
| −1 | 0 | 0 | 0 | 0 | 0 | 0 | 0 | 0 | 0 | 0 | 0 |
| −0.8 | 0 | 0 | 0 | 0 | 0 | 0 | 0 | 0 | 0 | 0 | 0 |
| −0.6 | 0 | 0 | 0 | 0 | 0 | 0 | 0 | 0 | 0 | 0 | 0 |
| −0.4 | 0 | 0 | 0 | 0 | 0 | 0 | 0 | 0 | 0 | 0 | 0 |
| −0.2 | 0 | 0 | 0 | 0 | 0 | 0 | 0 | 0 | 0 | 0 | 0 |
| 0 | 0 | 0 | 0 | −0.0096 | −0.0425 | 0.0000 | 0.0328 | 0 | 0 | 0 | 0 |
| 0.2 | 0 | 0 | 0 | −0.0244 | 0.0567 | 0.2356 | 0.0328 | 0 | 0 | 0 | 0.0269 |
| 0.4 | 0 | 0 | 0 | −0.0148 | 0.0992 | 0.2356 | 0 | 0 | 0 | 0 | 0.0269 |
| 0.6 | 0 | 0 | 0 | 0 | 0 | 0 | 0 | 0 | 0 | 0 | 0 |
| 0.8 | 0 | 0 | 0 | 0 | 0 | 0 | 0 | 0 | 0 | 0 | 0 |
| 1 | 0 | 0 | 0 | 0 | 0 | 0 | 0 | 0 | 0 | 0 | 0 |

**Table 9** Changes in the fuzzy rule-base for 2738kg at 0.1g Time 0.3sec

| e \ c | −1 | −0.8 | −0.6 | −0.4 | −0.2 | 0 | 0.2 | 0.4 | 0.6 | 0.8 | 1 |
|---|---|---|---|---|---|---|---|---|---|---|---|
| −1 | 0 | 0 | 0 | 0 | 0 | 0 | 0 | 0 | 0 | 0 | 0 |
| −0.8 | 0 | 0 | 0 | 0 | 0 | 0 | 0 | 0 | 0 | 0 | 0 |
| −0.6 | 0 | 0 | 0 | 0 | 0 | 0 | 0 | 0 | 0 | 0 | 0 |
| −0.4 | 0 | 0 | 0 | 0 | 0 | 0 | 0 | 0 | 0 | 0 | 0 |
| −0.2 | 0 | 0 | 0 | 0 | 0 | 0 | 0 | 0 | 0 | 0 | 0 |
| 0 | 0 | 0 | 0 | −0.0096 | −0.0425 | 0.0000 | 0.0328 | 0 | 0 | 0 | 0 |
| 0.2 | 0 | 0 | 0 | −0.0244 | 0.0567 | 0.2356 | 0.0328 | 0 | 0 | 0 | 0.0269 |
| 0.4 | 0 | 0 | 0 | −0.0148 | 0.0992 | 0.2356 | 0 | 0 | 0 | 0 | 0.0269 |
| 0.6 | 0 | 0 | 0 | 0 | 0 | 0 | 0 | 0 | 0 | 0 | 0 |
| 0.8 | 0 | 0 | 0 | 0 | 0 | 0 | 0 | 0 | 0 | 0 | 0 |
| 1 | 0 | 0 | 0 | 0 | 0 | 0 | 0 | 0 | 0 | 0 | 0 |

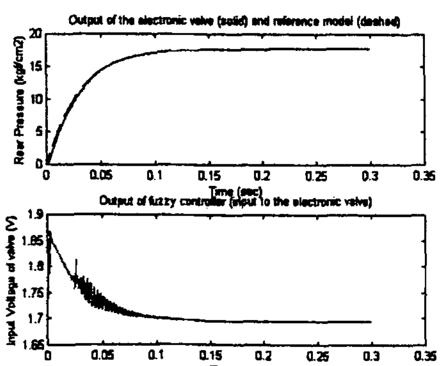


**Fig. 24** Simulation results of the direct adaptive fuzzy controller for 2738kg 0.1g

rule-base.

The brake line pressure distribution simulation results are shown in Figs. 34, 35 and 36. These simulation results show that a high rate of deceleration and a heavy weight condition cause a gap between the reference brake line pressure and the actual brake line pressure. The direct adaptive fuzzy algorithm method can reduce error quickly under all kinds of conditions.

## 4.2 Experimental results

### 4.2.1 Experimental results for the mechanical system

Considering the safety of the experiment, the vehicle was limited in its deceleration to 0.7g. So, deceleration of the vehicle increased from 0.1g to 0.7g. Figures 18, 19 and 20 show the braking force results for the empty weight condition, the half weight condition, and the gross weight condition during all rates of deceleration. At all three weight conditions, the rear wheel was not locked. However, this system has a large loss of braking forces. The reason for this is that the cut-in-pressure of the vehicle acts early, ahead of the designed cut-in-pressure. The L. S. P. V. was tested in order to prove its effectiveness in accordance with the service book. The results of the test show that the valve does not have good sensitivity for weight changes, and that it has assembly errors and manufacturing errors. So, the accuracy of assembling and manufacturing the valve affect the effectiveness of the L. S. P. V. in the mechanical system.

### 4.2.2 Experimental results for the electronic system

Figures 25, 26 and 27 show the experimental brake line pressure results of the electronic system with an 1840kg-weight condition using the direct adaptive fuzzy control method. These results show that reductions in rear brake line pressure start above 50kgf/cm², the reference cut-in-pressure of the electronic system. So, the rear brake line pressure is the same as the front brake line pressure when the value is below the reference cut-in-pressure. For decreasing rear brake line pressures, the valve slop of the electronic system is 0.07. The simulation of the electronic system progressed under the constant deceleration condition, but this condition could not be maintained because of trembling in the engine and chassis system of the experimental vehicle. The maximum low level deceleration is 0.19g, the maximum medium level deceleration is 0.59g, and the maximum high level deceleration is 0.74g.

Figures 28, 29 and 30 show the experimental brake line pressure results of the electronic system with a 2351kg-weight condition using the direct adaptive fuzzy control method. At that weight condition, the reference cut-in-pressure is 101kgf/cm² and the valve slop is 0.54. So, a

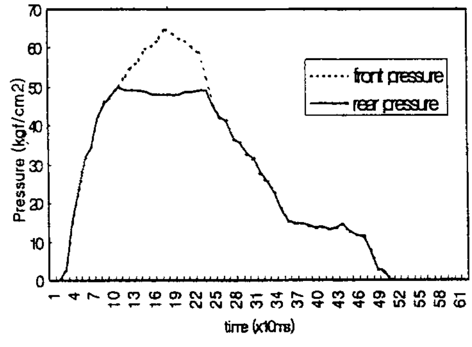


**Fig. 26** Experimental brake line pressure result of electronic system with 1840kg at medium level deceleration

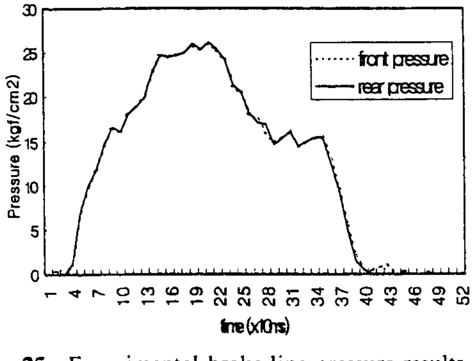


**Fig. 25** Experimental brake line pressure results for the electronic system for 1840kg at low level deceleration

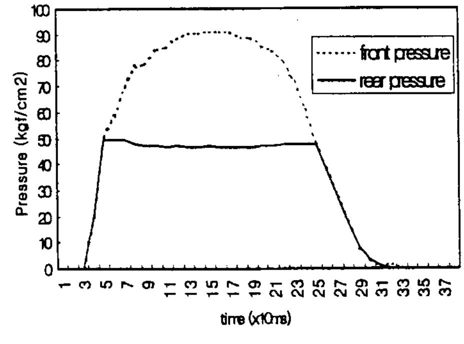


**Fig. 27** Experimental brake line pressure result of electronic system with 1840kg at High level deceleration

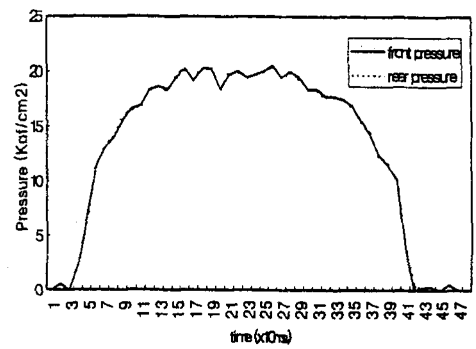


**Fig. 28** Experimental brake line pressure result of electronic system with 2351kg at low level deceleration

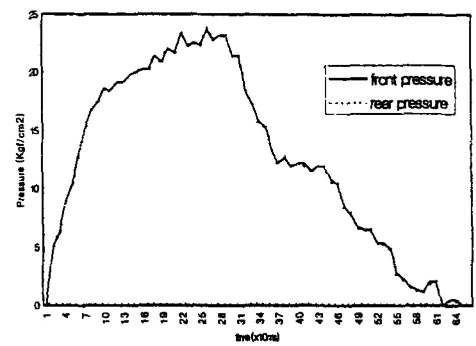


**Fig. 31** Experimental brake line pressure result of electronic system with 2738kg at low level deceleration

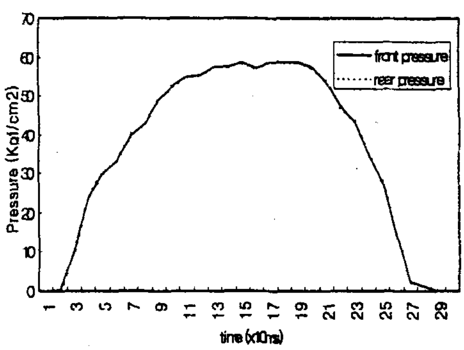


**Fig. 29** Experimental brake line pressure result of electronic system with 2351kg at medium level deceleration

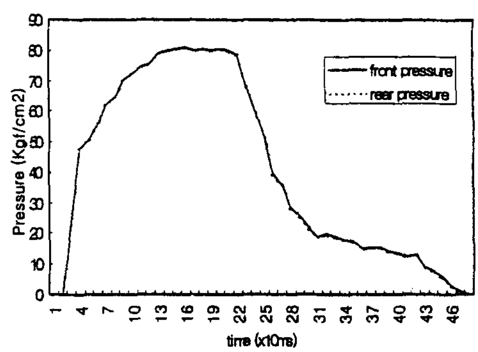


**Fig. 32** Experimental brake line pressure result of electronic system with 2738kg at medium level deceleration

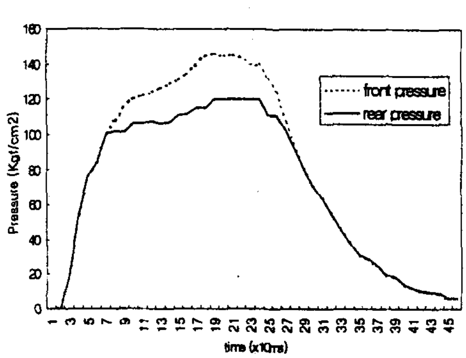


**Fig. 30** Experimental brake line pressure result of electronic system with 2351kg at high level deceleration

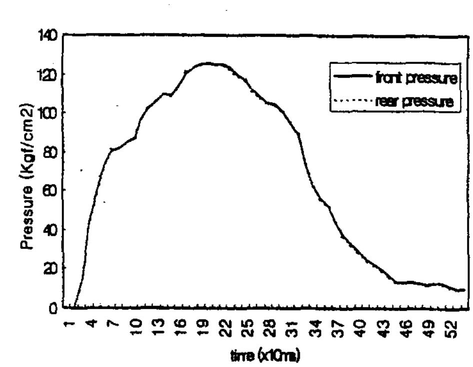


**Fig. 33** Experimental brake line pressure result of electronic system with 2738kg at high level deceleration

reduction in rear brake line pressure did not occur at the 0.15g low level deceleration and 0.39g medium level deceleration rates. However, a reduction in rear brake line pressure did not occur at the 0.89g high level deceleration rate.

Figures 31, 32 and 33 show the experimental brake line pressure results of the electronic system with a 2738kg-weight condition using the direct adaptive fuzzy control method. At that weight condition, the reference cut-in-pressure is

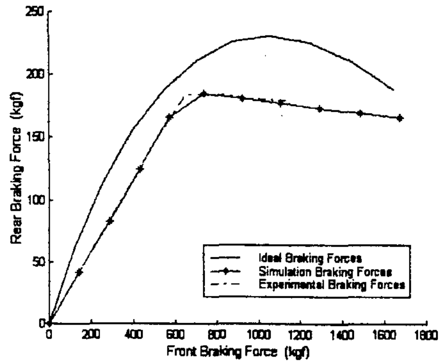


**Fig. 34** Electronic system results for 1840kg

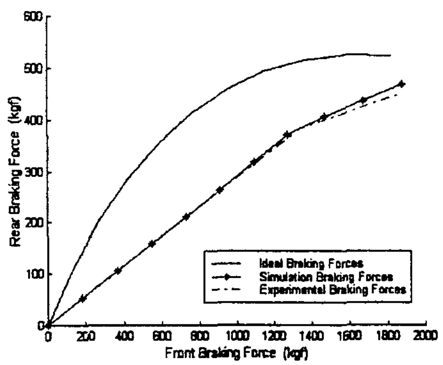


**Fig. 35** Electronic system results for 2351kg

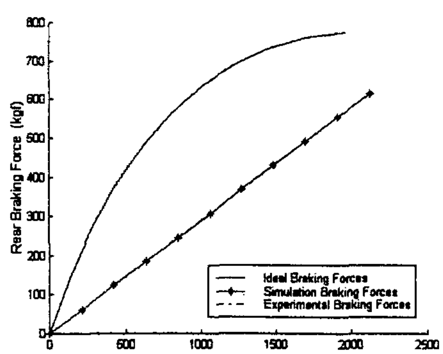


**Fig. 36** Electronic system results for 2738kg

140kgf/cm$^2$ and the valve slop is 1. So, reductions in rear brake line pressure did not occur at any deceleration level because the rear brake line pressure did not exceed the reference cut-in-pressure at that weight condition. Figures 34, 35 and 36 show the experimental braking forces results of the electronic system using the direct adaptive fuzzy algorithm method.

The above results all show a little error between the simulation of the electronic system using the direct adaptive fuzzy algorithm method and the experimental results of the same. The trembling of the experimental vehicle and the remaining air in the brake pipe seemed to affect the sensor and the E. C. U. in the reference output voltage of the reducing valve.

## 5. Conclusion

In this study, we proposed an electronic control of braking force distribution with a direct adaptive fuzzy controller to overcome the weaknesses of a mechanical system as follows:

(1) To overcome the a weaknesses of the mechanical system, we proposed a reference model for the direct adaptive fuzzy algorithm.

(2) To change the system from mechanical to electronic, we proposed a hardware system including sensors, a reducing valve, and a control unit.

(3) We proposed a direct adaptive fuzzy algorithm in which the fuzzy rule-base was changed depending on the deceleration conditions and weight conditions, and which had a closed loop control system. To accurately control the voltage of the electronic reducing valve, we studied the characteristics of the electronic valve and the mechanical system.

We anticipated that the electronic system, using the direct adaptive fuzzy control algorithm, could reduce the error between the reference pressure and the actual and could better overcome the loss of braking force than with the mechanical system because the electronic valve changed the cut-in-pressure and the valve slop simultaneously. As expected, the electronic system resulted in shorter braking distances than the mechanical system.

From an industrial viewpoint, the electronic system can be expected to have the following effects: The mechanical system needs many cut-in-pressures and valve slops to fit all kinds of vehicles. But the electronic system can be used universally to fit any kind of vehicle, sharing the hardware and changing only the software. So, automobile makers can reduce their effort and costs in the development of new valves.

In the future, if a new valve that can simultaneously control front and rear brake line pressure before reaching a reference cut-in-pressure is designed, we can expect greater reductions in the loss of brake line pressure than with the electronic systems studied in this paper.

## References


BOSCH, 1993, *Automotive Handbook*, Robert Bosch GmbH

Frederic, E. L., 1969, "Proportioning Valve to Skid Control-A Logical Progression," *SAE* Paper 690456.

Giuseppe, P., 1970, "Automatic Brake Proportioning Devices," *SAE* Paper 700375.

Gunther, B., 1992, "Electronic Brake force Distribution Control～A Sophisticated Addition to ABS," *SAE* Paper 920646.

Hiroyuki, N., 1977, "An Investigation of Braking Force Distribution," *JSAE* Vol. 31, No. 3

Jurgen, Ronald, 1997, *Automotive Electronics Handbook*, McGraw-Hill, Inc.

Kevin, M. P. and Stephen, Y., 1998, *Fuzzy Control*, An Imprint of Addison～Wesley Longman, Inc.

Kim, Y. S., 1997, "Present Technic and Future Trend of ABS," *KSAE* Vol. 19, No. 2, pp. 47～57.

Layne, J. R. and Kevin. M. P., 1993, "Fuzzy Model Reference Learning Control for Cargo Ship Steering," *IEEE Control Systems Magazine*, Vol. 13, No. 6, pp. 23～34.

Layne, J. R. and Kevin, M. P., 1996, *Fuzzy Model Reference Learning Control To appear in the Journal of Intelligent and Fuzzy Systems.*

Lefteri, H. T. and Robert, E. U., 1997, *Fuzzy and Neural Approaches in Engineering*, JOHN WILEY & SONS, INC.

Li-Xin, W., 1994, *Adaptive Fuzzy Systems and Control*, Prentice～Hall, Inc.

Mizutani, Shuji, 1992, *Car Electronics*, Nippondenso Co. Ltd.

Rudolf, L., 1971, "Proportional Braking of Solid Frame Vehicles," *SAE* Paper 710047.

Rudolf, L., 1974, "An Investigation of Brake Balance for straight and curved Braking," *SAE* Paper 741086.

Rudolf, L., 1992, *Brake Design and Safety*, Society of Automotive Engineers.

Thomas D. G., 1992, *Fundamentals of Vehicle Dynamics*, Society of Automotive Engineers.

Zadeh, L. A., 1973, "Outline of a New Approach to the Analysis of Complex Systems and Decision Processes," *IEEE Trans. on Systems, Man, and Cybern.*, SMC～3, No. 1, pp. 28～44.

Zadeh, L. A., 1985, "Syllogistic Reasoning in Fuzzy Logic and Its Application to Usuality and Reasoning with Dispositions," *IEEE Trans. on Systems, Man, and Cybern.*, SMC～15, No. 6, pp. 754～763.